result is that the two models produced nearly identical cloud feedback, as shown by their similar λ/λ_c values (Table 2). Nor is it possible to segregate the 14 GCMs into low- and high-sensitivity groups on the basis of whether they do or do not incorporate cloud optical properties that depend upon cloud water content. The ECMWF and ECMWF/UH GCMs also incorporate this effect, and they lie at opposite ends of the cloud feedback spectrum (Table 2). Furthermore, even though the CSU and OSU/LLNL GCMs produced nearly identical modest positive cloud feedback (Table 2), this was actually a result of compensation between vastly different cloud feedback components.

In summary, although the 14 atmospheric GCMs produced comparable clear-sky sensitivity parameters, when cloud feedback was included, compatibility vanished and there was a nearly threefold variation in climate sensitivity as produced by the models. The cloud feedback ranged from modest negative to strong positive feedback. Clearly improvements in the treatment of clouds in GCMs are needed. But there are many other facets of a GCM, in addition to cloud optical properties and cloud formation parameterizations, that can influence cloud-climate interactions. The hydrological cycle, to cite one example, will most certainly play a dominant role.

Many of these GCMs are in a continual state of evolution. Thus this intercomparison is a snapshot that might no longer represent a specific model. Furthermore, these model-produced cloud feedbacks may not be representative of how the models would behave under realistic climate change conditions when they are coupled with interactive cryosphere and ocean models. Perpetual July simulations cannot be used for this purpose. Nor can the uniform SST perturbations, because they do not account for changes in equator-to-pole temperature gradients associated with actual climate change. For example, it has recently been speculated (*10*) that this latter effect, by itself, may produce a cloud feedback component resulting from latitudinal shifts in general circulation patterns. But these caveats do not alter our conclusion that 14 different GCMs produced a broad spectrum of cloud-climate feedback.

Climate research benefits from a diversity of climate models. If only a limited number of models were available, we could not confidently conclude that the role of cloud feedback is a key issue for climate studies. Before this study, only two GCMs had been used to provide estimates of cloud feedback (*5, 6*), and these two estimates showed much closer agreement than we have demonstrated.

REFERENCES AND NOTES

1. M. E. Schlesinger and J. F. B. Mitchell, *Rev. Geophys.* **25**, 760 (1987).
2. R. D. Cess and G. L. Potter, *J. Geophys. Res.* **93**, 8305 (1988).
3. Another important cause of these differences is that different climate models produce different control (that is, present-day) climates. For example, see (*2*); M. J. Spelman and S. Manabe, *J. Geophys. Res.*, **89**, 57 (1984).
4. R. E. Dickinson, in *Carbon Dioxide Review*, W. C. Clark, Ed. (Clarendon, New York, 1982), pp. 101–133; G. L. Potter and R. D. Cess, *J. Geophys. Res.* **89**, 9521 (1984).
5. R. T. Wetherald and S. Manabe, *J. Atoms. Sci.* **45**, 1397 (1988).
6. J. Hansen *et al.*, in *Climate Processes and Climate Sensitivity*, J. E. Hansen and T. Takahashi, Eds. (American Geophysical Union, Washington, DC, 1984), pp. 130–163. Hansen *et al.* indicated a feedback amplification due to clouds of 1.3 in their GCM study, but this value is for the absence of other feedback mechanisms. When water vapor and snow-ice feedbacks were included, their results implied a cloud feedback amplification of 1.8.
7. R. D. Cess, *J. Atmos. Sci.* **33**, 1831 (1976).
8. S. Manabe and R. T. Wetherald, *ibid.* **24**, 241 (1967).
9. T. P. Charlock and V. Ramanathan, *ibid.* **42**, 1408 (1985); V. Ramanathan, *J. Geophys. Res.* **92**, 4075 (1987).
10. V. Ramanathan *et al.*, *Science* **243**, 57 (1989).
11. R. C. Alexander and R. L. Mobley, *Mon. Weather Rev.* **104**, 143 (1976).
12. V. K. Petukhov *et al.*, *Izv. Acad. Sci. U.S.S.R. Atmos. Oceanic Phys.* **11**, 802 (1975); R. C. J. Somerville and L. A. Remer, *J. Geophys. Res.* **89**, 9668 (1984); M. E. Schlesinger, *Nature* **333**, 303 (1988).
13. A brief description of the 14 GCMs will be provided in Cess *et al.* (in preparation); descriptions of individual models are available from the respective investigators.

14. Valuable insights and suggestions were provided by W. L. Gates and M. E. Schlesinger. This study represents one of several Department of Energy model intercomparison projects, and it was performed under the auspices of the CO_2 Research Division, Office of Basic Energy Sciences, U.S. Department of Energy contract W-7405-ENG-48 to Lawrence Livermore National Laboratory, grant DEFG0285ER60314 to SUNY Stony Brook, and contract DE-AI01-80EV10220 to the National Center for Atmospheric Research, which is sponsored by the National Science Foundation. Further support was provided by the National Aeronautics and Space Administration Climate Program grant NAG 5-1058 to Colorado State University, and by the Bundeminister für Forschung and Technologie, Federal Republic of Germany, grant KF20128 to the University of Hamburg.

10 March 1989; accepted 20 June 1989

β-Adrenergic Inhibition of Cardiac Sodium Channels by Dual G-Protein Pathways

BERND SCHUBERT, ANTONIUS M. J. VANDONGEN, GLENN E. KIRSCH, ARTHUR M. BROWN

The signaling pathways by which β-adrenergic agonists modulate voltage-dependent cardiac sodium currents are unknown, although it is likely that adenosine 3′5′-monophosphate (cAMP) is involved. Single-channel and whole-cell sodium currents were measured in cardiac myocytes and the signal transducing G protein G_s was found to couple β-adrenergic receptors to sodium channels by both cytoplasmic (indirect) and membrane-delimited (direct) pathways. Hence, G_s can act on at least three effectors in the heart: sodium channels, calcium channels, and adenylyl cyclase. The effect on sodium currents was inhibitory and was enhanced by membrane depolarization. During myocardial ischemia the sodium currents of depolarized cells may be further inhibited by the accompanying increase in catecholamine levels.

IN THE LEXICON OF NEUROMODULATION, voltage-dependent Na^+ channels receive far less attention than voltage-dependent K^+ or Ca^{2+} channels, possibly because of the all-or-none nature of the propagated action potential. Previous studies, however, have shown that (i) the β-adrenergic agonist isoproterenol (ISO) decreases maximum upstroke velocity in depolarized ventricular myocytes (*1*); (ii) cAMP-dependent phosphorylation reduces neurotoxin-activated $^{22}Na^+$ flux (*2*) and promotes inactivation in embryonic rat brain cells (*2*); and (iii) cAMP modulates Na^+ currents in frog node of Ranvier (*2*). These studies suggest that a signal transducing G protein may link β-adrenergic receptors to Na^+ channels. To test this possibility, we examined the effects of ISO on Na^+ currents by whole-cell and single-channel recording in neonatal ventricular myocytes from rat.

ISO (1 μ*M*) applied extracellularly reduced whole-cell Na^+ current (I_{Na}) by 40.8 ± 17.5% (mean ± SD, $n = 4$) when I_{Na} was partially inactivated at a holding potential (HP) of −60 mV (Fig. 1A). The decrease began without measurable delay, was half maximal at about 5 s, peaked at about 15 s (Fig. 1A), and occurred without an

B. Schubert, Department of Molecular Physiology and Biophysics, Baylor College of Medicine, One Baylor Plaza, Houston, TX 77030, and Division of Cellular and Molecular Cardiology, Central Institute for Cardiovascular Research, Academy of Sciences of the GDR, Berlin-Buch, GDR.
A. M. J. VanDongen, G. E. Kirsch, A. M. Brown, Department of Molecular Physiology and Biophysics, Baylor College of Medicine, One Baylor Plaza, Houston, TX 77030.

obvious change in kinetics (Fig. 1A, inset). However, when I_{Na} was fully activatable (HP = −90 mV), ISO even at much higher concentrations (40 μ*M*) applied for longer times (3 min) produced a decrease of only 3.6 ± 1.4% (Fig. 1B) (n = 5). The same concentration applied for the same time but at a HP of −60 mV produced a reduction of 51 ± 22% (n = 5). On the basis of the dependence of the ISO effect on HP, we hypothesized that ISO reduced the availability of Na^+ channels for activation by acting preferentially on inactivated channels (*3*). Therefore, we measured the voltage dependence of steady-state inactivation (h_∞) from a HP of −60 mV and found that ISO produced a shift of −18 ± 5 mV (n = 4) in the midpoint of the curve relating h_∞ to membrane potential [h_∞ (V) curve] (Fig. 1C). However, at a HP of −90 mV this shift was only −7 ± 3 mV (n = 5). Hence, ISO acts like a local anesthetic in that it shifts the h_∞ (V) curve to more negative potentials and is more effective when the membrane is held in a depolarized state (*4*).

The effect of ISO on the Na^+ current was partially reversible after washing ISO out of the bath (Fig. 1A) (n = 4). A complication was that the availability of the Na^+ current decreases with time in whole-cell patch clamp experiments (*5*). The shift of the h_∞ (V) curve decreased I_{Na} amplitude by itself, and this inhibition overlapped with the inhibition produced by ISO. The shift was most pronounced when large patch pipettes (0.5 to 1 megohm) were used and, with such pipettes, we estimated an upper limit of the shift that might occur under control conditions. In six experiments at a HP of −60 mV the midpoint shifted at an average rate of 0.9 ± 0.6 mV/min and would have produced an average reduction in I_{Na} of 6% per minute, which was much smaller than the reductions produced by ISO (Fig. 1A). In addition, the shift in the h_∞ (V) curve was much less for the smaller (1.5 to 5 megohm) pipettes we actually used in the ISO experiments.

To test whether the ISO effect involved G proteins, which are present in the heart (*6*), we replaced guanosine triphosphate (GTP) in the patch pipette with guanosine 5′-*O*-2-thiodiphosphate (GDPβS), a nonhydrolyzable guanosine diphosphate (GDP) congener. GDPβS at 2 m*M* prevented the ISO inhibition (Fig. 1D), and 3 min after application of ISO the decrease in I_{Na} at —60 mV was only 13.7 ± 5.7% (n = 4). These results suggested that the ISO effect may be via a G protein, possibly G_s, acting through either the cytoplasmic cAMP cascade as in cardiac Ca^{2+} channels (*7*) or through a membrane-delimited, direct pathway as in muscarinic atrial K^+ channels (*8*), neuronal K^+ channels (*8*), and Ca^{2+} channels in cardiac and skeletal muscle (*8*).

We tested the involvement of the cAMP cascade in the ISO effect by recording single-channel Na^+ currents in cell-attached patches and adding ISO to the solution bathing the cell membrane outside the patch. The single-channel currents were reduced by 37 ± 11% (n = 5) when h_∞ was about 0.5, and the reduction was abolished when h_∞ was 1.0 (Fig. 2A). If cAMP acted as a second messenger in the effect of ISO, the membrane-permeable cAMP analog 8-bromo—cAMP should mimic the ISO result. In four experiments, 8-bromo–cAMP at 50 to 400 μ*M* was added to the bath outside the membrane patch and, at a h_∞ of 0.5, inhibited the single-channel currents by 35 ± 12%. In two whole-cell current experiments at a HP of −60 mV ($h_\infty \simeq 0.5$) 8-bromo–cAMP reduced I_{Na} by 39 and 41%. Thus ISO acts via a cytoplasmic cAMP pathway, and this pathway is more effective when the membrane is depolarized.

To test for the involvement of the direct membrane-delimited pathway, we measured single-channel Na^+ currents from excised inside-out membrane patches. With ISO at 10 μ*M* in the pipette, inhibition did not occur until GTP (200 μ*M*) was added to the bath (Fig. 2B). The GTP-dependent inhibition occurred in 7 of 12 experiments and at a conditioning potential of −120 mV, where $h_\infty \simeq 0.5$, was 75 ± 14.5%. This effect was also voltage-dependent and could be partially reversed by hyperpolarizing prepulses to −150 mV (n = 5). The lack of inhibition in five experiments with $h_\infty \simeq 0.5$ might have been due to the absence of β-adrenergic receptors or activatable G protein in the patch. GTP (1 to 2 m*M*) produced less than 10% inhibition without ISO in the pipette in five experiments.

In a preferred method of agonist-independent activation of endogenous G proteins (*9*) we used the nonhydrolyzable GTP analog guanosine 5′-*O*-(3-thiotriphosphate) (GTPγS). In the absence of ISO in the pipette, GTPγS in the bath decreased the single-channel Na^+ currents to 4.3 ± 2.6% (n = 6) of the control value. The inhibition required Mg^{2+}, further supporting the involvement of an endogenous G protein; in the absence of Mg^{2+} and the presence of GTPγS, the opening probability of single-channel Na^+ currents was 85.7 ± 9.5% (n = 4) of control. GTP (2 m*M*) prevented the inhibitory effect of 400 μ*M* GTPγS, suggesting competition for a GTP binding site. The nonhydrolyzable adenosine triphosphate (ATP) congener adenosine 5′-*O*-(3-thiotriphosphate) (ATPγS) (400 μ*M*) had a small effect (n = 3), possibly due to conversion of ATPγS to GTPγS by a nucleotide diphosphate kinase (*10*). Thus, our data indicated that ISO could inhibit whole-cell and single-channel Na^+ currents by both indirect and direct pathways. The direct effect seemed to be more pronounced (compare Fig. 2A with Fig. 2B) and, like the

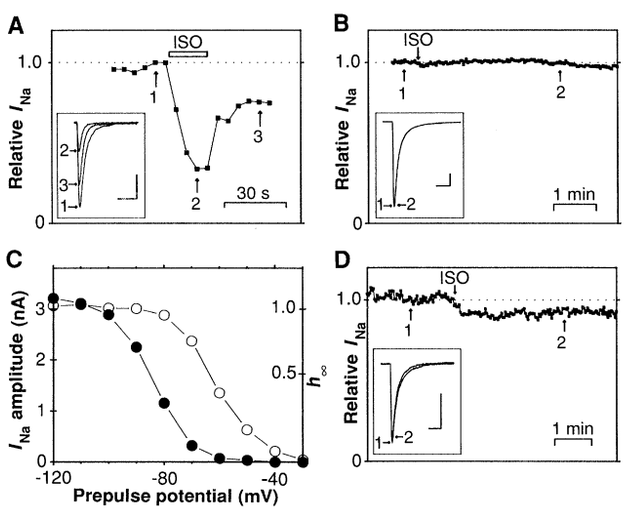

Fig. 1. Inhibition of cardiac Na^+ currents by ISO: dependence on membrane potential and guanine nucleotides. Whole-cell Na^+ currents from neonatal rat cardiac myocytes (*17*) were produced by depolarizing test pulses to 0 mV from various HPs applied for 55 ms at 0.5 Hz in (B), (C), and (D) and at 0.2 Hz in (A) (*18*). (**A**) ISO (1 μ*M*) inhibits the normalized (to 1) peak amplitude of whole-cell Na^- currents (I_{Na}) at a HP of −60 mV. The peak amplitude was the difference between the peak and the steady current at the end of the pulse. ISO was present as indicated by the bar, which was shifted by 5 s to correct for the measured delay of our perfusion system. GTP (500 μ*M*) was present in the pipette solution. (Inset) Current traces taken at times indicated. Calibrations, 3.0 ms and 500 pA. (**B**) ISO (40 μ*M*) has almost no effect on the peak amplitude of Na^+ currents at a HP of −90 mV. ISO was applied at the arrow. Test pulses, 0.5 Hz; GTP, 500 μ*M*. (Inset) As in (A). (**C**) ISO shifts the Na^+ channel inactivation curve. The peak amplitude of the Na^+ current produced by a test pulse to 0 mV (this is an index of h_∞) is plotted as a function of the potential of a 200-ms conditioning prepulse; HP, −60 mV. (○) Control; (●) 40 μ*M* ISO. The lines are the fits of the data by a Boltzmann equation. Fifty percent inactivation of the Na^+ channel (h_∞ = 0.5) was at −64 ± 2 mV (n = 4) and at −82 ± 6 mV (n = 4), before and after ISO application, respectively. (**D**) Effect of GDPβS (2 m*M*) on inhibition of Na^+ currents produced by 40 μ*M* ISO at a HP of −60 mV. ISO applied as in (B). (Inset) As in (A).

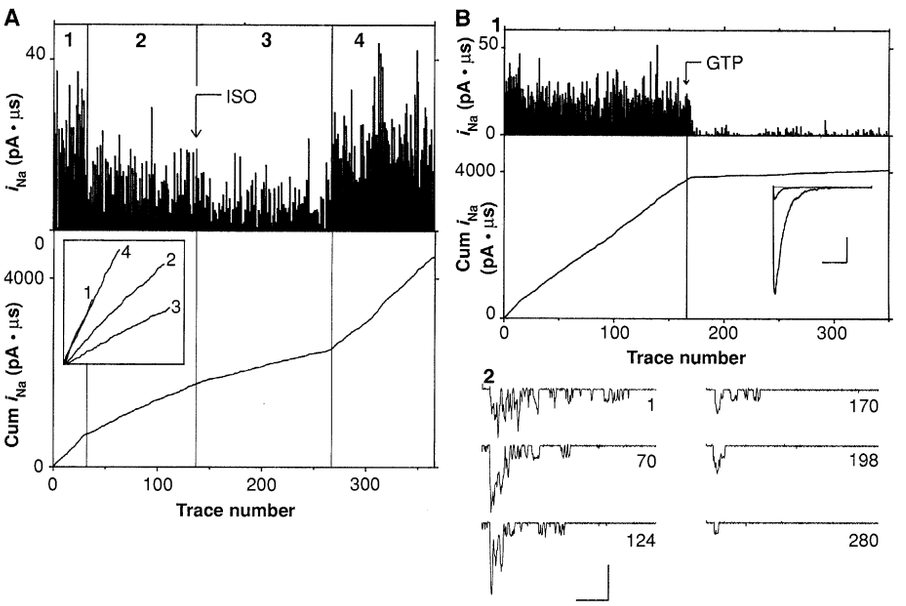

Fig. 2. ISO inhibition of single-channel Na^+ currents by (A) second messenger and (B) direct pathways. (**A**) Inhibition of Na^+ currents by ISO via a second messenger pathway. Single-channel Na^+ currents were recorded from a cell-attached membrane patch. The pipette solution contained 137 m*M* NaCl, 5.4 m*M* KCl, 1 m*M* $MgCl_2$, 2 m*M* $CaCl_2$, 10 m*M* glucose, 10 m*M* Hepes, (*p*H 7.4 adjusted with NaOH) (290 mOsm). To zero the resting potential, the bathing solution was 140 m*M* potassium aspartate, 2 m*M* $MgCl_2$, 5 m*M* EGTA, 5 m*M* Hepes (*p*H adjusted to 7.4). HP throughout the experiment was −100 mV which, for cell-attached patches, set h_∞ to about 0.5 (*5*). In the upper section single-channel Na^+ currents in each trace were integrated and plotted as a function of trace number. The integral was chosen because it is a reliable measure of channel activity in multichannel patches. A cumulative plot of the integrated currents is shown in the lower section. For sections 1 and 4, depolarizing test pulses were preceded by 200-ms hyperpolarizing prepulses to −150 mV to fully remove inactivation. In 2 and 3, the hyperpolarizing prepulses were omitted. ISO at 10 μ*M* was added at the arrow. (Inset) The cumulative plots for 1 to 4 with the starting point moved in each case to a common origin. The slopes (in pA·μs per trace) were, by linear least squares analysis, 21.9, 10.3, 5.6, and 21.0, respectively. The inhibition produced by ISO in 3 was removed by turning on the prepulse in 4. (**B**) GTP reconstitutes the inhibition produced by ISO in inside-out patches. Single-channel Na^+ currents were recorded from excised inside-out membrane patches of neonatal rat ventricle cells in primary culture. The bathing solution contained 110 m*M* CsOH, 110 m*M* aspartic acid, 20 m*M* $CsCl_2$, 2 m*M* $MgCl_2$, 5 m*M* EGTA, 5 m*M* Hepes (*p*H 7.3 adjusted with CsOH) (290 mOsm). ISO at 10 μ*M* was in the pipette solution and GTP at 200 μ*M* was added to the bathing solution at the arrow. Each trace was produced by depolarizing steps of 55 ms to −60 mV, which were applied at 0.5 Hz from HP of −90 mV. h_∞ was adjusted to about 0.5 which, due to the hyperpolarizing shift of h_∞ in inside-out patches (*5*), required 200-ms prepulses to −120 mV. (**B_1**) In the upper section integrated single-channel Na^+ currents are plotted as a function of trace number. In the lower section is a cumulative plot of the integrated currents as a function of trace number from the same patch. (Inset) The sum of the individual current traces before and after addition of GTP. The two traces could be scaled, indicating that the kinetics were not changed. Calibrations, 10 ms and 2 pA. (**B_2**) Representative records are shown before (left) and after (right) application of GTP. Calibrations, 10 ms and 5 pA.

indirect effect, was greater when the membrane was depolarized.

Since G_s couples β-adrenergic receptors to Ca^{2+} channels and adenylyl cyclase, it was the leading G protein candidate for the inhibitory effect (*11*). To test this, we examined whether human erythrocyte G_s preactivated with GTPγS (G_s^*) could simulate the effect of ISO plus GTP or the effect of GTPγS on inside-out patches in the absence of substrate. This was the case in four of four experiments, with G_s^* at 100 to 200 p*M* (Fig. 3, A and B). The results were specific for G_s^*; G_k, the human erythrocyte G protein [which when preactivated with GTPγS (G_s^*) activated single muscarinic atrial K^+ channel currents (*8*)] had no effects at concentrations up to 200 p*M* (n = 3) (Fig. 3, C and D), and a preactivated bovine brain G protein preparation (containing 60% G_o and several G_i's) [which activated neuronal K^+ currents (*12*)] was also ineffective (n = 3). A cholera toxin substrate with the electrophoretic properties of $G_s\alpha$ is present in heart (*6*), and we conclude that ISO plus GTP or GTPγS activated an endogenous G protein that is similar to human erythrocyte G_s and that this G_s can inhibit Na^+ channels directly.

The voltage dependence of the ISO effect involves a hyperpolarizing shift of inactivation that resembles the shift that occurs in response to local anesthetics (*13*) and, like local anesthetic block, the effect is strongly potentiated by depolarized holding potentials (*14*). Agents that inhibit inactivation such as pronase, α-scorpion toxin, and a site-directed antibody (*15*) also act in a voltage-dependent manner but, unlike the G protein effect, they are less effective when the membrane is held at more positive potentials.

Our conclusions are that (i) voltage-gated cardiac Na^+ channels are directly and indirectly modulated by G_s; (ii) a single G protein may have as many as three effectors; in this case G_s modulates Na^+ channels,

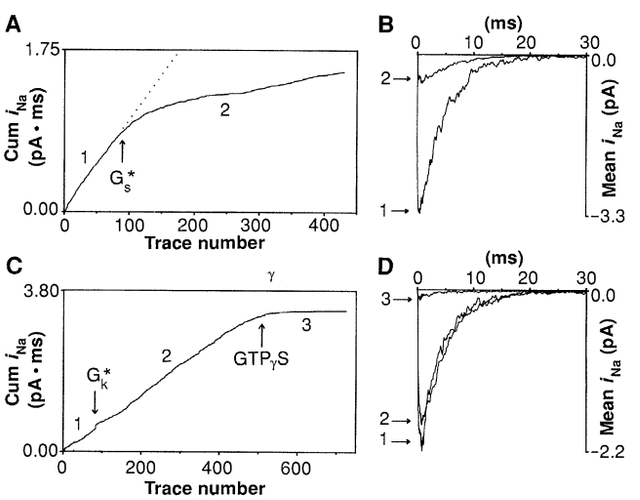

Fig. 3. Inhibition by G_s^* but not G_k^* (*19*) of single-channel Na^+ currents in excised inside-out patches from neonatal rat ventricular myocytes. Depolarizing steps of 55 ms to −50 mV were applied at 0.5 Hz from a HP of −90 mV. Test pulses were preceded by 200-ms prepulses to −140 mV. (**A**) Single-channel Na^+ currents during each trace were integrated and plotted cumulatively against trace number as in Fig. 2. Preactivated G_s^* (100 p*M*) was added to the bathing solution on the intracellular side of the membrane. (**B**) The idealized single-channel currents in each trace of (A) were summed and divided by the number of traces for the periods before (1) and after (2) application of preactivated G_s^* (**C**) Cumulative plot as in (A). Preactivated G_k^* (200 p*M*) was added to the bathing solution (arrow). Later, GTPγS (200 μ*M*) was added (arrow). (**D**) The idealized currents in each trace of (C) were summed (1) before, (2) after application of G_s^*, and (3) after application of 400 μ*M* GTPγS.

Ca^{2+} channels, and adenylyl cyclase. Thus, G proteins, in addition to acting as signal transducers, can link different effectors into membrane networks; (iii) in the heart β-adrenergic agonists produce opposite changes in I_{Ca} and I_{Na}, but the effects on I_{Na} require that the membrane potential is depolarized. These effects will be exaggerated in the ischemic myocardium because ischemia causes membrane depolarization through extracellular K^+ accumulation and is accompanied by an increased catecholamine concentration (*16*). Thus, our results may explain the data linking high levels of catecholamine to a greater risk of severe arrhythmias associated with myocardial infarction.

REFERENCES AND NOTES

1. M. Windisch and H. Tritthart, *J. Mol. Cell. Cardiol.* **14**, 431 (1982); I. Hisatome, T. Kiyosme, S. Imanishi, M. Arita, *ibid.* **17**, 657 (1985).
2. W. A. Catterall, *Science* **242**, 50 (1988); T. L. Seelig and J. J. Kendig, *Brain Res.* **245**, 144 (1982).
3. A. L. Hodgkin and A. F. Huxley, *J. Physiol. (London)* **117**, 500 (1952). The inactivated state is a closed state favored by depolarization from which the channels cannot be activated. It differs in this way from the resting, closed state. In this context, inactivation and unavailability of channels are used interchangeably.
4. A. M. Brown and A. Yatani, *The Heart and Cardiovascular System* (Raven Press, New York, 1986), vol. 1, p. 627.
5. E. Fenwick, A. Marty, E. Neher, *J. Physiol. (London)* **331**, 599 (1982); J. M. Fernandez, A. P. Fox, S. Krasne, *ibid.* **356**, 565 (1984); D. L. Kunze *et al.*, *J. Gen. Physiol.* **86**, 691 (1985).
6. N. M. Scherer *et al.*, *Arch. Biochem. Biophys.* **251**, 431 (1987); S. W. Halvorsen and N. M. Nathanson, *Biochemistry* **23**, 5813 (1984).
7. H. Reuter, *Nature* **301**, 569 (1983); M. Kameyama *et al.*, *Pfluegers Arch.* **405**, 285 (1985).
8. A. Brown *et al.*, *Cold Spring Harbor Symp. Quant. Biol.* **53**, 365 (1988).
9. R. Cerione *et al.*, *Biochemistry* **26**, 1485 (1987).
10. A. Otero *et al.*, *Science* **242**, 443 (1988).
11. L. Birnbaumer *et al.*, *Kidney Int.* **32**, S14 (1987); A. G. Gilman, *Annu. Rev. Biochem.* **56**, 615 (1987).
12. A. M. J. VanDongen *et al.*, *Science* **242**, 1433 (1988).
13. B. I. Khodorov, *Prog. Biophys. Mol. Biol.* **374**, 49 (1981).
14. B. Hille, *J. Gen. Physiol.* **69**, 494 (1977).
15. V. L. Salgado, J. Z. Yeh, T. Narahashi, *Biophys. J.* **47**, 567 (1985); W. A. Caterall, *J. Gen. Physiol.* **74**, 375 (1979); P. M. Vassilev, T. Scher, W. A. Catterall, *Science* **241**, 1658 (1988).
16. A. Wollenberger and L. Shaab, *Nature* **207**, 88 (1965); H. J. Hirche *et al.*, *J. Mol. Cell. Cardiol.* **12**, 579 (1980).
17. Primary cardiac cell cultures were prepared from hearts of 1- to 3-day-old neonatal rats [G. E. Mark and F. F. Strasser, *Exp. Cell Res.* **44**, 217 (1966)] and used as described in Kunze *et al.* (*5*).
18. We used the patch-clamp technique [O. P. Hamill, A. Marty, E. Neher, B. Sakmann, F. J. Sigworth, *Pfluegers Arch.* **391**, 85 (1981)] to record whole-cell and single-channel Na^+ currents that had the gating, conductance, and pharmacological properties that have been reported for fast cardiac Na^+ channels (*4*). For whole-cell measurements we selected small spherical cells (10 μm in diameter) with membranes that behaved as a simple resistance-capacitance (*R-C*) circuit with a time constant <100 μs [D. L. Kunze *et al.*, in (*5*)]. Test potentials were always on the positive limb of the current-voltage (*I-V*) curve and the currents had none of the features of inadequate space clamp. Patch pipettes had tip resistances of 1.5 to 5.0 megohms and the input resistance of the cells was about 1.0 gigaohm. Capacitive transient cancellation and series resistance adjustments were made to provide optimum settling and attenuation of the capacitive current transient.

Currents were digitized and recorded at 44 kHz on a pulse-code modulated videocassette recorder for off-line analysis. Before digitization, currents were filtered at 5 kHz (−3 dB) with a 4-pole Bessel filter. The data were then transferred to a MicroVax II computer for further analyses. No corrections for leak currents were made for whole-cell recordings. The single-channel records were filtered before analysis with a Gaussian finite-impulse response filter.

The experimental chamber (200 to 500 μl) was placed on an inverted microscope stage. When necessary, external solutions were superfused at 2 ml per minute by gravity. To suppress outward currents, the pipettes were filled with a Cs^+-rich solution of 118 m*M* CsOH, 118 m*M* aspartic acid, 6.4 m*M* $MgCl_2$, 5 m*M* EGTA, 4.2 m*M* ATP, 2.7 m*M* $CaCl_2$, 5 m*M* Hepes, *p*H 7.3 with CsOH (290 mOsm adjusted with cesium aspartate). The calculated free concentrations of Mg^{2+} and Ca^{2+} were 2 m*M* and 0.1 μ*M*, respectively. After breaking the patch, the pipette solution was allowed to equilibrate with the cell interior for a few minutes. The external solution contained 137 m*M* NaCl, 5.4 m*M* KCl, 1 m*M* $MgCl_2$, 2 m*M* $CaCl_2$, 5 m*M* $CoCl_2$, 10 m*M* glucose, 10 m*M* Hepes, *p*H 7.4, adjusted with NaOH (290 mOsm). Ca^{2+} currents were suppressed by addition of Co^{2+} in the presence of Mg^{2+}. All experiments were performed at 20° to 22°C.
19. The G proteins used in this study were purified from human erythrocyte membranes to greater than 95% purity (as assessed by Coomassie blue staining) by fractionation techniques that yield G_s essentially free of G_k and G_k essentially free of G_s [A. Yatani *et al.*, *J. Biol. Chem.* **263**, 9887 (1988)].

20. Supported in part by NIH grants HL36930 and HL39262 to A.M.B. We thank L. Birnbaumer and J. Codina for G proteins (DK19319 and HL31164 to L. B.) and J. Breedlove, D. Witham, and V. Price for their secretarial assistance.

3 March 1989; accepted 23 May 1989

The Effect of Deprenyl (Selegiline) on the Natural History of Parkinson's Disease

JAMES W. TETRUD AND J. WILLIAM LANGSTON

The effects of MPTP (1-methyl-4-phenyl-1,2,3,6-tetrahydropyridine), a neurotoxin that produces the symptoms of Parkinson's disease, can be fully prevented in experimental animals by inhibiting monoamine oxidase B. On the basis of this observation, a double-blind, placebo-controlled study in patients with early Parkinson's disease was initiated to determine whether deprenyl (a selective monoamine oxidase B inhibitor) would delay the need for L-dopa therapy by slowing the progression of the disease. Fifty-four patients were randomly assigned to deprenyl (10 mg/day) or placebo treatment groups and followed until L-dopa therapy was indicated or until the patient had been in the study for 3 years. Analysis of Kaplan-Meier survival curves for each group showed that deprenyl delayed the need for L-dopa therapy; the average time until L-dopa was needed was 312.1 days for patients in the placebo group and 548.9 days for patients in the deprenyl group. Disease progression, as monitored by five different assessment scales, was slowed (by 40 to 83% per year) in the deprenyl group compared to placebo. Therefore, early deprenyl therapy delays the requirement for antiparkinsonian medication, possibly by slowing progression of the disease.

PARKINSON'S DISEASE IS INVARIABLY progressive. Although drugs for symptomatic treatment are available, none slow the progress of the disease. L-Dopa remains the backbone of modern treatment, but complications, toxicity, and decreased effectiveness tend to appear with long-term use of all antiparkinsonian drugs or with progression of the disease (*1*). For these reasons, there is a critical need for a new treatment aimed at retarding disease progression.

In 1983, two seemingly unrelated events set the stage for the therapeutic trial reported here. First, Birkmayer and colleagues (*2*) reported that parkinsonian patients receiving both L-dopa and the selective monoamine oxidase (MAO) inhibitor, deprenyl, appeared to live longer than patients receiving L-dopa alone. They surmised that deprenyl might be preventing death of neurons in the substantia nigra, the central neuropathological feature in Parkinson's disease, thus slowing disease progression. Their report provoked little response, perhaps because it was retrospective in nature. That same year, we published an account of four young drug abusers who developed pure parkinsonism after using a new "synthetic heroin"; the offending agent was tentatively identified as 1-methyl-4-phenyl-1,2,3,6-tetrahydropyridine (MPTP) (*3*). MPTP was quickly shown to be selectively toxic to the substantia nigra in both rhesus (*4*) and squirrel monkeys (*5*), thus providing a striking pathological analogy to Parkinson's disease. After the discovery that MAO

California Parkinson's Foundation, 2444 Moorpark Avenue, Suite 316, San Jose, CA 95128.